JACS
JOURNAL OF THE AMERICAN CHEMICAL SOCIETY
Perspective
pubs.acs.org/JACS

Conducting Polymer-Based Catalysts

Qinqin Zhou and Gaoquan Shi*

Department of Chemistry, Tsinghua University, Beijing 100084, People's Republic of China

ABSTRACT: Conducting polymers (CPs) have been widely applied as electrocatalysts and photocatalysts in energy-related systems, sensors, and environmental protection. This is mainly due to their promising catalytic activities, high conductivities, and unique electrochemical and optical properties. Furthermore, CPs can be cheaply and conveniently prepared in large scale via chemical or electrochemical approaches. In this Perspective, we review the recent advancements on the synthesis and applications of CP-based inherent and composite catalysts and CP-derived heteroatom-doped carbon catalysts. The mechanisms of catalysis will be introduced, and the challenges of developing CP-based catalysts with practical importance will be discussed.

1. INTRODUCTION

Conducting polymers (CPs) have unique one-dimensional (1D) delocalized conjugated structures and excellent electrical, electrochemical, and optical properties; thus they have been widely explored as inherent electrocatalysts and photocatalysts.[1,2] Specifically, the high conductivity and electroactive properties of CPs make them be able to catalyze the redox reactions involved in dye sensitized solar cells (DSSCs), fuel cells, and biosensors, etc.[3−9] CPs usually possess narrow and tunable bandgaps. Consequently, they can absorb UV−vis and/or near-infrared lights, suggesting they are promising photocatalysts or photosensitizers with activities upon illumination with solar light.[10−14] Furthermore, many CP catalysts have good biocompatibility and can be easily fabricated into flexible films or nanostructures, facilitating their applications in biosystems and flexible devices.[15−17] CPs are also conductive supports for immobilizing other catalysts to improve their performances or extend their functions.[7,9] Both inherent and composite CP catalysts can be chemically or electrochemically synthesized in the forms of powders and films.[15] The CP-based films are able to be directly used as catalytic electrodes,[17] and their powders have to be loaded to the surfaces of conductive current collectors with polymeric binders for electrocatalysis.[18] CP-based photocatalysts are powders, and they are usually used without further treatments.[11] To enhance the activity and/or improve the stability of CP catalysts, they also have to be nanostructured[16,19,20] or blended with cocatalysts[12,21] and/or other highly conductive components.[22] CP catalysts are cheap and effective and can be easily obtained in large scale. These facts explain why CPs have important applications in catalysis, having been extensively studied in recent years. However, an article that systematically summarizes the researches on CP-based catalysts has not yet been published. This Perspective aims to review the recent advancements on the synthesis and applications of CP catalysts, introduce the catalytic mechanisms, and discuss the challenges of developing CP-based catalysts with practical importance. To limit the length of this article, we selected typical CP catalysts and catalytic systems as examples, so many excellent papers are possibly not included. This Perspective gives an outline of this interesting and important field.

2. CP-BASED ELETROCATALYSTS

Electrocatalysts should have high electrical conductivities, large specific surface areas, and electroactive properties.[4,23] CPs satisfy these requirements and have been widely explored for the catalyzation of I^-/I_3^- redox reaction in DSSCs,[3,4,6,17,19,20,22,24−32] oxygen reduction reaction (ORR) in fuel cells,[7,18,33−40] and redox reactions in biosensors,[8,16,21,41−45] etc. The typical CPs used for electrocatalysis include polyaniline (PANI), polypyrrole (PPy), polythiophene (PTh), and its derivatives, especially, poly(3,4-ethylenedioxythiophene) (PEDOT).

Catalytic Electrodes of DSSCs. A conventional DSSC has a dye-sensitized TiO_2 photoanode, an electrolyte containing I^-/I_3^- ions, and a catalytic counter electrode.[46] The functions of its counter electrode include collecting electrons from the external circuit and catalyzing the redox reaction of I^-/I_3^-. Platinum (Pt) has been confirmed to be an effective catalytic counter electrode of the DSSC with I^-/I_3^- mediator.[3] However, Pt suffers from high cost and the rarity of its natural resources. CPs together with carbon materials (e.g., carbon nanotube and graphene) and non-noble metal compounds have been explored to replace Pt.[4] Among these alternatives, CPs have attracted much attention because of their encouraging electrocatalytic activity, high conductivity, ease of synthesis, and controllable nanostructures. Furthermore, the good transparency and flexibility of ultrathin CP films make them a more promising catalytic electrode for bifacial and flexible DSSCs.[17,47]

The mechanism of CP-based catalyzation toward the redox reaction of I^-/I_3^- has not yet been clearly revealed. Nevertheless, a possible explanation has been proposed: I^- and I_3^- ions weakly or strongly bonded to CP backbones via van der Walls, π-electron and/or electrostatic interactions.[24] The formation of charge-transfer complexes at the interface of CP electrode and electrolyte as well as inside CP matrix decreases the activation energy of I^-/I_3^- redox reaction.[48] Taking PPy as an example (Figure 1),[24] PPy···I^- and PPy···I_3^- or PPy−I^- and PPy−I_3^- represent the weakly or strongly bonded complexes. The dissociation of PPy···I_3 and the adsorption of I_2 molecules on the N atoms of PPy produce an electric neutral intermediate

Received: November 29, 2015
Published: February 10, 2016

DOI: 10.1021/jacs.5b12474
J. Am. Chem. Soc. 2016, 138, 2868−2876

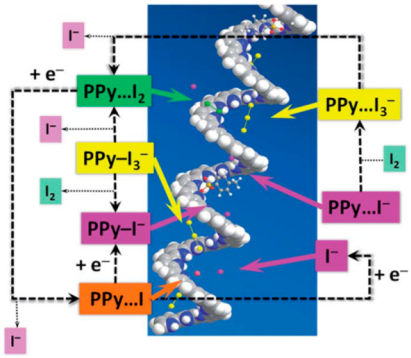

Figure 1. Proposed electrocatalytic mechanism of PPy electrode toward the reduction of I_3^- ions. Reprinted with permission from ref 24. Copyright 2014, RSC Publishing.

of PPy···I_2. During the electrocatalytic process, this intermediate is further reduced to I^- ions. The weakly bonded complexes (e.g., PPy···I_3^-) are the dominant elctrocatalytic sites, while the strongly bonded complexes (doping) increase the conductivity of PPy. Both of them facilitate the reduction of I_3^- to I^-. The electron-transfer from I^- ions to excited dye molecules leads to regenerate the dye.

In order to optimize the electrocatalytic performances of CP catalysts, their specific surface areas and conductivity should be maximized.[19,20,25−28] A larger specific surface area provides CP catalyst with more exposed active sites for enhancing its catalytic activity. For this purpose, CPs were usually nanostructured by choosing different doping ions,[25,26] using hard[19] or soft templates[20] in their synthesis processes. For example, PEDOT nanotubes (Figure 2a) were electrochemically synthesized using pre-electrodeposited ZnO nanowires on fluorine-doped tin oxide (FTO) glass sheet as a template, followed by removing the template with acid.[19] The DSSC with a counter electrode of these PEDOT nanotubes displayed a high power conversion efficiency (PCE) of 8.3%, higher than that of the counterpart with a flat PEDOT film (7.9%) (Figure 2b). In another work, PEDOT nanofibers (Figure 2c) with diameters of 10−50 nm were chemically prepared using sodium dodecyl sulfate (SDS) as a soft template (or nanoreactors).[20] Successively, PEDOT fibers dispersed in a methanol/dimethyl sulfoxide (DMSO) cosolvent were spin-coated on FTO sheet and used as the counter electrode of DSSC, showing a PCE (9.2%) much higher than that of bulk PEDOT-based DSSC (6.8%), even surpassing the corresponding Pt-based DSSC (8.6%) (Figure 2d).

The conductivities of CPs are another key factor of controlling their electrocatalytic performances. High conductivity is beneficial for the charge transfer at the interface between electrolyte and counter electrode, accelerating the reduction of I_3^-. Several techniques can be applied to increase

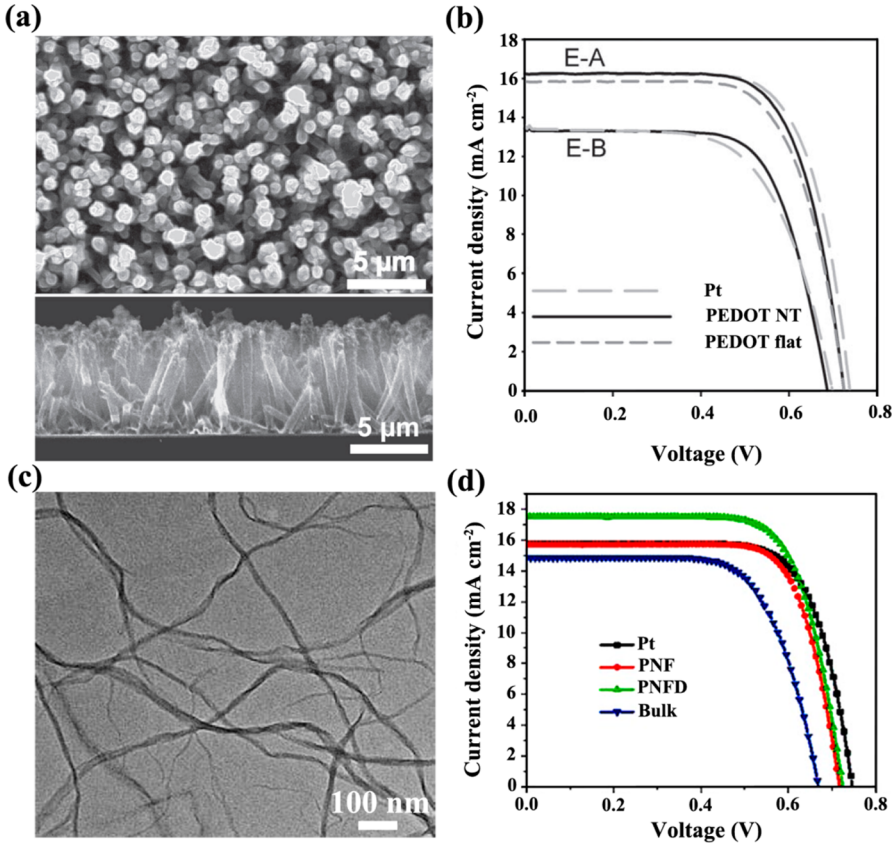

Figure 2. (a) Top view and cross-section scanning electron micrographs of PEDOT nanotube (NT) counter electrode. (b) Photocurrent density−photovoltage (J−V) curves of Pt, PEDOT NT, and flat PEDOT film counter electrodes based DSSCs using different electrolytes (E-A is I^-/I_3^- electrolyte dissolved in acetonotrile:valeronitrile (85:15 vol %), and E-B is I^-/I_3^- electrolyte dissolved in methoxypropionitrile solvent). Reprinted with permission from ref 19. Copyright 2011, Wiley-VCH. (c) Transmission electron micrograph of PEDOT nanofibers. (d) J−V curves of the DSSCs using different counter electrodes: Pt, PEDOT nanofibers (PNF), methanol/DMSO cosolvent treated PEDOT nanofibers (PNFD), and bulk PEDOT. Reprinted with permission from ref 20. Copyright 2012, RSC Publishing.

DOI: 10.1021/jacs.5b12474
J. Am. Chem. Soc. 2016, 138, 2868−2876

the conductivities of CPs, such as modulating their doping ions and doping levels,[26,27] treating them with solvents,[49−53] and adding conductive additives.[22] For example, *p*-toluenesulfonate-doped PEDOT (PEDOT-TsO) was synthesized via a chemical approach. It has a conductivity (550 S cm^{-1}) much higher than that of polystyreneslufonate-doped PEDOT (PEDOT-PSS) (10 S cm^{-1}), resulting in a higher PCE for the PEDOT-TsO-based DSSC.[27] In this case, the partial exchange of small TsO^- anions with I^-/I_3^- ions also improved the catalytic performance of PEDOT-TsO electrode. The conductivity of commercially available PEDOT:PSS can be increased to about 1000 S cm^{-1} by treating it with DMSO,[28] ethylene glycol, or hexafluoroacetone[50] and even up to 4380 S cm^{-1} by using concentrated sulfuric acid.[51] Very recently, Wu's group fabricated PEDOT:PSS modified FTO electrodes by repeatedly spin-coating an aqueous solution of PEDOT:PSS containing 10% (by volume) DMSO and successively annealing on a hot plate.[28] The thickness of one-layer spin-coated PEDOT:PSS film was about 70 nm. The conductivity of an one-layer or five-layer PEDOT:PSS film increased from 0.07 S cm^{-1} for one-layer untreated PEDOT:PSS (the solvent of its dispersion was pure water) to 724 or about 950 S cm^{-1}. In this case, the DMSO in the cosolvent induced a phase separation of conductive PEDOT and insulated PSS domains, enhancing the crystallization of conjugated PEDOT chains. As a result, the DMSO-treated PEDOT-PSS films have greatly increased conductivities. Actually, the DMSO-treated five-layer PEDOT:PSS-based DSSC achieved the highest PCE of 9.01%, much higher than that of untreated one-layer PEDOT:PSS-based device (4.52%), and comparable to that of Pt-based counterpart (9.77%). The improved catalytic performances of PEDOT electrodes were mainly attributed to their enhanced electrical conductivities and the formation of nanoporous fibrillary morphology. DMSO-treated PEDOT:PSS film has also been used to replace FTO conductive substrate, the PCE of corresponding DSSC was reported to be as high as 8.29%.

The conductivities of CP catalysts can be improved by blending highly conductive carbon nanomaterials such as carbon nanotubes and graphene.[22,29,54] Furthermore, carbon nanomaterials are able to construct three-dimensional (3D) conductive frameworks for immobilizing CP catalysts.[22,29] The carbonaceous frameworks can provide the catalytic electrodes with highly conductive channels and large specific surface areas. A typical example is using the network of multiwall carbon nanotubes (MWCNTs) prepared by electrophoresis on a FTO electrode to load ClO_4^- ion-doped PEDOT by pulse potentiostatic polymerization.[22] This PEDOT/MWCNT-based DSSC exhibited a PCE of 7.03%, higher than those of PEDOT- (6.39%), MWCNTs- (1.07%), and even Pt-based (5.88%) DSSCs. Very recently, a nitrogen-doped graphene (NGr)/Nafion slurry was drop casted on FTO and used as a continuously conductive matrix, followed by the electrodeposition of PEDOT.[29] This PEDOT/NGr-based DSSC exhibited a higher PCE (8.30%) than that of the counterpart with PEDOT (6.96%), NGr (6.54%), or Pt (8.17%) electrode.

The transparency and flexibility of CP catalytic electrodes make them have unique applications in bifacial and flexible DSSCs.[17,29,47] A bifacial DSSC can be illuminated by light from both front and rear sides to improve its performance. Flexible DSSCs have attracted more attention, because they are suitable for mass-production through a roll-to-roll process and can be used to build integrated photovoltaics. In 2010, Pringle et al. paved the first step to fabricate flexible DSSC with a counter electrode fabricated by electrodepositing PEDOT on a ITO/polyethylene naphthalate (ITO/PEN) conductive substrate.[17] The corresponding solar cell exhibited a high PCE of 8.0%. This PEDOT electrode can be prepared at room temperature by electrochemical polymerization for only 5 s, making it to be cost-effective and time-saving.

Several metal compounds (e. g., CoS,[30] TiN[31] nanoparticles) have also been blended to PEDOT:PSS to form composite catalysts with improved performances. One typical example was a TiN/PEDOT:PSS composite electrode prepared by doctor blading a viscous mixture of TiN nanoparticles and the aqueous dispersion of PEDOT:PSS.[31] The DSSC with this catalytic electrode showed a PCE of 7.06%, exceeding those of PEDOT:PSS- (2.04%), TiN- (0.76%), and Pt-based (6.57%) DSSCs. This improved performance was attributed to the introduction of additional TiN active sites and the formation of a conductive network of PEDOT:PSS.

Except for the I^-/I_3^- electrolyte, PEDOT can also catalyze the redox reactions of disulfide/thiolate (T_2/T^-) and Co^{2+}/Co^{3+} mediators in DSSCs. Co^{2+}/Co^{3+} mediator has a higher redox potential, and the DSSC with this electrolyte has a higher open circuit voltage (V_{OC}) compared with the counterpart with I^-/I_3^-.[55] So far, the DSSC with a PEDOT counter electrode, Co^{2+}/Co^{3+} electrolyte, and Y123 dye was reported to have the highest PCE of 10.30%.[32]

ORR Catalysts. ORR involved in fuel cells or metal-air batteries is a sluggish reaction to control the whole process of oxidizing a chemical fuel (e.g., H_2, methanol, or ethanol) or a metal (e.g., Zn or Al) to generate electric power.[56] Pt has been tested to be the best catalyst toward ORR. However, the high cost, drift phenomenon (releasing Pt nanoparticles from electrode), and easy toxifying by carbon oxide (CO, an intermediate product of electro-oxidizing alcohol fuels) of the Pt catalyst strongly limit its practical applications.[33] CPs have been explored as alternative ORR catalysts because of their good electrocatalytic activity, high conductivity, and satisfactory electrochemical stability. CP-based ORR catalysts include inherent CPs, CP composites and CP-derived heteroatom-doped carbons.

The catalytic mechanism of inherent CP catalysts has been explained from two aspects: (1) A neutral CP is an electron donor, and O_2 is an electron acceptor. Thus, CP can strongly interact with the O_2 molecules adsorbed on its surface via charge transfer, activating the latter by decreasing its molecular symmetry and increasing the lengths of O═O bonds. Quantum chemical calculations also suggested that an O_2 molecule was activated through bonding its oxygen atoms to the two adjacent carbon atoms around a nitrogen atom of PANI (side on model).[18] (2) CPs naturally remained in a mildly oxidized form in the electrochemical cell. The O_2 molecules adsorbed on the surface of a CP catalyst can further oxidize CP chains to a higher oxidation degree, while themselves are reduced into O^{2-} anions.[33]

A conventional CP electrode was fabricated through the following procedures: chemically synthesized CP powders were blended with a poly(tetrafluoride ethylene) binder, and then the paste was casted on a graphite current collector.[18] However, the ORR reaction catalyzed by this type of electrodes was kinetically slow with low electron-transfer efficiency, following a two-electron reaction pathway (reducing O_2 to H_2O_2 via combining two protons) in an acid medium. This phenomenon is probably due to the poor conductivity of neutral CPs. Increasing the conductivity and specific surface area of a CP

DOI: 10.1021/jacs.5b12474
J. Am. Chem. Soc. 2016, 138, 2868−2876

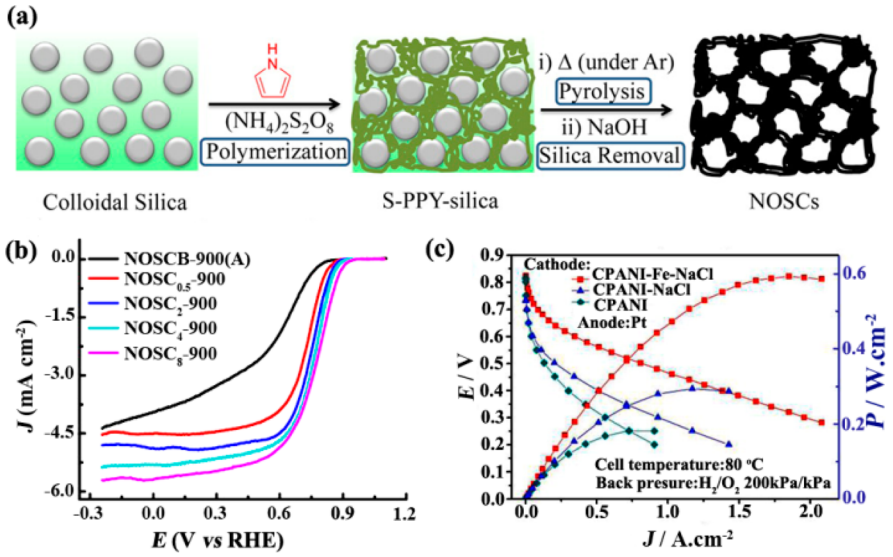

Figure 3. (a) Schematic illustration of preparing N-, O-, and S-tridoped nanoporous carbons (NOSC) from PPy. (b) Polarization curves of $NOSC_x$-900 °C catalysts (x represents the amount of colloidal silica template) coated on rotating disk electrodes at a rotating speed of 1600 rpm in an oxygen-saturated 0.1 M KOH solution. Reprinted with permission from ref 37. (c) Polarization curves and power densities of the PEMFCs with CPANI-Fe-NaCl, CPANI-NaCl, and CPANI cathodes, respectively. Reprinted with permission from ref 39.

catalyst can increase its catalytic performance. For example, Winther-Jensen and co-workers reported a conductive and nanostructured PEDOT electrode via a vapor-phase polymerization method using iron(III) *p*-toluenesulfonate (Fe(III)PTS) as oxidant and porous Goretex film as substrate.[33] Impressively, this PEDOT electrode displayed high catalytic activities for ORR in the electrolytes with a broad range of pH values, strong tolerance toward CO poison, and a long-term stability for more than 1500 h. A trace amount of residual Fe in this catalyst could also accelerate ORR. The authors tried to exclude the effect of Fe on ORR based on CO poison test. However, this is insufficient, because Fe active sites probably cannot be poisoned by CO as reported by other researchers;[57] thus further study is needed to exclude Fe effect.

The incorporation of metal active centers into CP matrices is an effective approach to improve the catalytic performances of inherent CPs. Taking the work by Bashyam and Zelenay as an example.[34] In this case, PPy was chosen as a matrix of cobalt (Co^{σ}, $0 \le \sigma \le +2$) to mimic the Co−N atomic configuration in a cobalt porphyrin. This catalyst was prepared by chemical polymerization of pyrrole with H_2O_2 on Vulcan XC-72 and followed by loading Co atoms via reducing $Co(NO_3)_2$. It was nominated as Co-PPy-C, and its performance was tested in a H_2-O_2 polymer electrolyte membrane fuel cell (PEMFC). This PEMFC generated a current density of about 0.2 A cm^{-2} at 0.50 V with a maximum power density around 0.14 W cm^{-2}. However, the ORR reaction catalyzed by this pyrolysis-free Co−PPy−C catalyst mainly followed a two-electron reaction pathway with a slow reaction rate.

CP-derived heteroatom-doped carbons were also tested to be effective ORR catalysts. Since Dai et al. reported that nitrogen (N)-doped carbon nanotubes showed strong catalytic activity toward ORR in 2009,[58] N-doped carbon catalysts have been widely studied. PANI and PPy are N-containing polymers; thus they were frequently pyrolyzed to produce N-doped carbon catalysts. The nitrogen atoms doped in carbon lattice mainly have four bonding configurations: pyrrolic N, quaternary N (or graphitic N), pyridinic N, and pyridine-N-oxide.[59] Pyridinic-N atoms have been widely regarded as the active sites of catalysis, because their delocalized p electrons facilitate the reductive adsorption of O_2 molecules. The carbon atoms that are neighbors to pyridinic-N atoms are positively charged, providing N-doped carbon with a strong catalytic activity for ORR. On the other hand, the graphitic-N atoms in the carbon lattice facilitate the electron transfer from the carbon conductive bands to the antibonding orbitals of O_2, also enhancing the ORR catalytic activity of N-doped carbon.[60,61]

CP-derived carbon codoped with N and other heteroatoms (e.g., B, O, S and P, etc.) showed improved performances on ORR due to their increased asymmetrical atomic spin density.[35−37] For example, Dai et al. prepared a N, P codoped mesoporous carbon by pyrolysis of a PANI aerogel synthesized in the presence of phytic acid.[36] The ORR at this catalyst showed an onset potential (0.94 V vs reversible hydrogen electrode, RHE) comparable to that at Pt/C in an O_2-saturated 0.1 M KOH solution. Theoretical calculation also indicated that the minimum overpotential of N, P codoped graphene for ORR is 0.44 V, slightly lower than that of Pt (about 0.45 V). Asefa and co-workers prepared N-, O-, and S- tridoped nanoporous carbons (NOSCs) by carbonizing the PPy powders synthesized via oxidizing pyrrole with $(NH_4)_2S_2O_8$ in the presence of a template of colloidal silica nanoparticles (Figure 3a).[37] It displayed a high onset potential of ORR (0.96 V vs. RHE), strong current density, and a four-electron process (reducing a O_2 molecule to $4OH^-$ via combining $2H_2O$) in an O_2-saturated 0.1 M KOH solution (Figure 3b). This encouraging performance is even superior to those of some excellent metal-based ORR catalysts reported in literature.

The incorporation of transition-metal (Fe, Co, Mn) active centers is another effective method to increase the catalytic performance of N-doped carbon.[38,39,62,63] In this case, metal-nitrogen (M-N) active sites were formed, and the metal additives also catalyzed the carbonization reaction.[62] The catalytic mechanism of M-N active sites is similar to that of metal porphyrins.[63] At the beginning, an O_2 molecule interacts with a metal atom to form a σ-bond via electron donation from the π-orbital of oxygen to the empty d-orbitals of metal. Successively, the partial electron is transferred back from metal

DOI: 10.1021/jacs.5b12474
J. Am. Chem. Soc. 2016, 138, 2868−2876

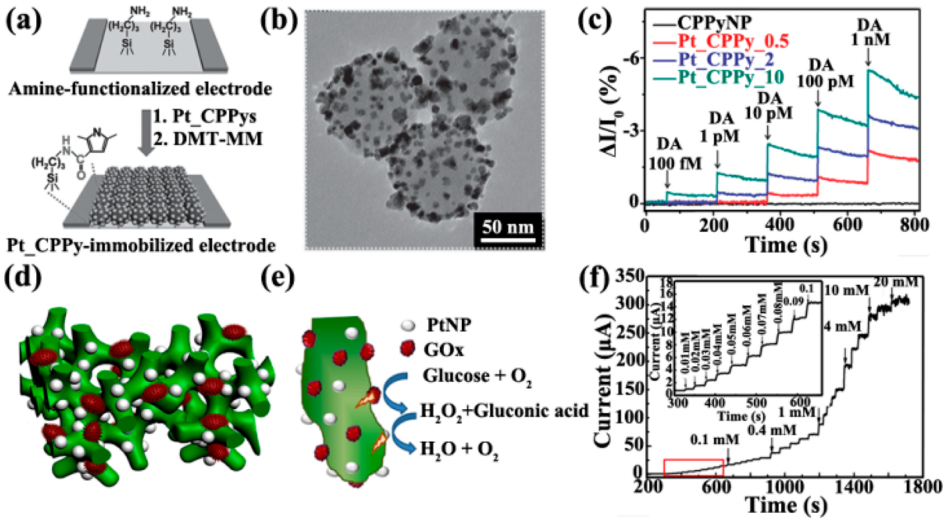

Figure 4. (a) Schematic illustration of fabricating Pt_CPPy modified interdigitated microelectrode. (b) TEM images of Pt_CPPy. (c) Normalized current changes with real-time for the Pt_CPPy electrode-based FETs with different densities of Pt particles. Reprinted with permission from ref 43. Copyright 2015, Wiley-VCH. (d) Schematic diagram of the 3D heterostructure of enzyme/PtNP/PANI hydrogel. (e) The proposed reaction mechanism of the GOx/PtNP/PANI hydrogel based sensor for glucose. (f) Amperometric response toward glucose with different concentrations in 0.1 M PBS (pH = 5.6) by GOx/PtNP/PANI hydrogel electrode at a potential of 0.56 V (vs saturated calomel electrode). Inset: a magnified curve of the part cycled by red rectangle. Reprinted with permission from ref 45.

d-orbitals to the antibonding π-orbital of oxygen. The activated complex can significantly decrease the bonding energy of O_2, thus facilitating ORR.[64] Furthermore, the formation of the strong O-metal bonds is favorable for the dissociation of a O_2 molecule into two oxygen atoms, leading the ORR to follow the four-electron process (reducing a O_2 molecule to two H_2O molecules via combining with four protons in acidic media).[63] Müllen et al. prepared a mesoporous carbon containing N and Fe atoms (C-N-Fe) from a polyaniline−Fe complex using silica colloids (12 nm) as the template.[38] The ORR catalyzed by C-N-Fe exhibited a high onset potential (0.84 V vs. RHE) with an electron-transfer number of 3.95 at 0.5 V in an O_2-saturated 0.5 M H_2SO_4 solution. The Fe−N_x bonds in this catalysts are reorganized as the main catalytic sites. Recently, Wei and co-workers initiated a novel "shape fixing via salt recrystallization" method to prepare a mesoporous C-N-Fe catalyst with enhanced activity.[39] $FeCl_3$ was immobilized on the networks of chemically synthesized PANI nanofibers. This PANI nanofiber/$FeCl_3$ composite was dispersed in an 80 °C supersaturated NaCl solution, followed by recrystallization of NaCl. This NaCl crystal sealed composite was pyrolyzed and washed with acid to produce a Fe-, N-containing carbon catalyst. It was nominated as CPANI-Fe-NaCl, and its content of Fe was measured to be 3.18 atom %. In this case, NaCl sealed nanoreactors enhanced the contacts of PANI fibers and Fe ions and increased the N content of CPANI-Fe-NaCl (5.85%). Actually, this N content was about twice that of PANI-derived N-carbon (CPANI, 3.04%). The ORR catalyzed by CPANI-Fe-NaCl showed a half-wave potential only 58 mV lower than that of Pt/C in an O_2-saturated 0.5 M H_2SO_4 solution. The PEMFC with a CPANI-Fe-NaCl cathode and a Pt anode generated a high peak power density of 600 mW cm^{-2} (Figure 3c), indicating CPANI-Fe-NaCl is one of the best nonprecious metal catalysts for ORR.

In addition, the incorporation of binary metals into a N-doped carbon can further improve its catalytic performance, especially its electrochemical stability. Zelenay et al. mixed aniline oligomer with Ketjen-black carbon nanoparticles and metal precursors ($Co(NO_3)_2$ and/or $FeCl_3$), followed by chemical polymerization and pyrolysis.[40] The most active PANI-FeCo-C exhibited an onset potential of ORR at about 0.93 V, and this value is comparable to that of PANI−Fe-C in an O_2-saturated 0.5 M H_2SO_4 solution. More importantly, the PEMFC with PANI-FeCo-C cathode kept stable for 700 h at a voltage of 0.4 V, showing a much weaker self-discharging current density (18 $\mu A\ h^{-1}$) compared with that of PANI−Fe-C-based PEMFC (90 $\mu A\ h^{-1}$).

CP Catalysts for Electrochemical Sensors. Since 1980s, CPs have been widely applied as electrodes for fabricating electrochemical sensors because of their high conductivity, unique electrochemical activity, biocompatibility, and controllable nanostructures.[8] The important parameters of evaluating an electrochemical sensor are its sensitivity, response rate, selectivity, and stability. The sensitivity of a CP-based electrochemical sensor depends on its catalytic activity, specific surface area, conductivity, and device configuration. CPs can be used as inherent catalysts or conductive supports for enzymes in electrochemical sensors.

Inherent CP catalysts have weak activities toward many target molecules, such as hydrogen peroxide (H_2O_2), dopamine (DA), ascorbic acid (AA), and uric acid (UA). Thus, nanoparticles of precious metals (e.g., Au, Pt) or carbon nanomaterials have frequently been introduced to increase their conductivities and catalytic activities.[41,42] Typically, Zhu et al. prepared PANI/Au hollow spheres by using polystyrene/sulfonated polystyrene core−shell particles as a template.[41] The PANI/Au modified glassy carbon electrode (GCE) exhibited a lower overpotential and stronger catalytic current toward the oxidation of DA compared with those of pure PANI or Au modified GCE. This is mainly due to that Au nanoparticles improved the charge transfer between the target molecules and PANI matrix. Similarly, carbon nanotubes were loaded on the surface of a PEDOT-coated GCE.[42] This CNT/PEDOT composite modified electrode showed stronger electrocatalytic currents of reducing H_2O_2 and oxidizing DA, AA, and UA without interference compared with those at a PEDOT

DOI: 10.1021/jacs.5b12474
J. Am. Chem. Soc. 2016, 138, 2868−2876

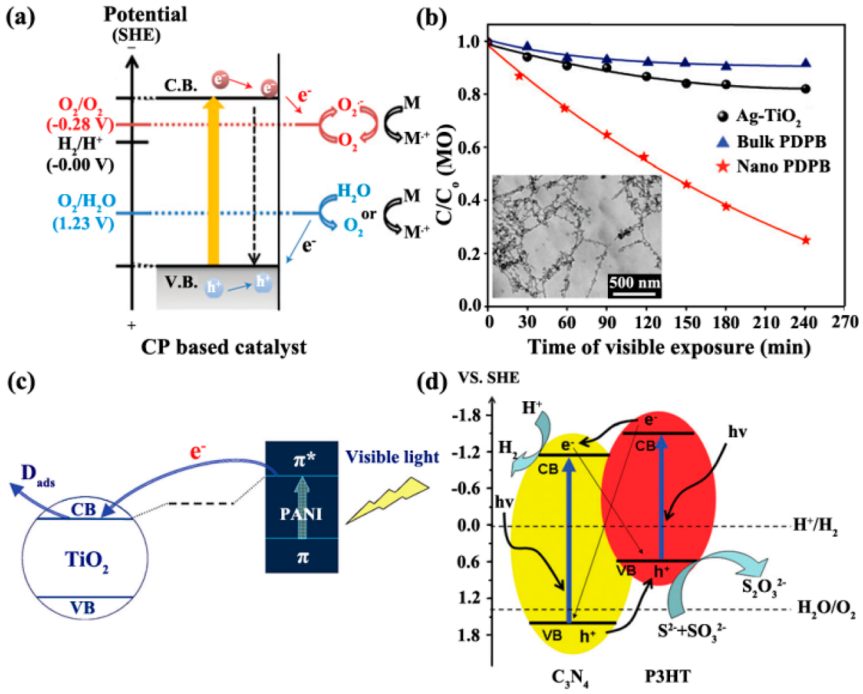

Figure 5. (a) Mechanism scheme of photodecomposition of pollutants by a CP-based catalyst. (b) Photocatalytic degradation of methyl orange using Ag-TiO_2, bulk PDPB, and nano PDPB photocatalysts. Inset: Transmission electron micrograph of PDPB nanofibers. Reprinted with permission from ref 11. Copyright 2015, Nature Publishing. (c) Mechanism scheme of a PANI/TiO_2 photocatalyst toward the degradation of pollutants under visible light. Reprinted with permission from ref 68. (d) Scheme of proposed mechanism of producing H_2 from water using a P3HT/g-C_3N_4 photocatalyst under visible light. Reprinted with permission from ref 12. Copyright 2011, RSC Publishing.

modified electrode. Meanwhile, this composite modified electrode was electrochemically stable even after storing for more than one month in 0.1 M PBS solution.

To enhance the sensitivities of CP-based sensors, field-effect transistors (FETs) with amplification ability were fabricated to replace traditional amperometric sensors. In FETs, CPs act as the supports of metal catalysts and transducers. In a recent report, carboxylated polypyrrole (CPPy) particles were covalently bonded to the surface of an interdigitated microelectrode array, followed by modifying Pt nanoparticles (Figure 4a,b).[43] This Pt/CPPy FET sensor displayed a high sensitivity toward DA with an extremely low limit of detection (100×10^{-15} M) and excellent selectivity (Figure 4c). In this case, Pt nanoparticles catalyzed the oxidation of DA, and the generated electrons neutralized the holes in CPPy (a p-type transducer) to give a response of current decreasing. The enhanced sensitivity of this sensor was attributed to the high catalytic activity of Pt nanoparticles and the amplification of FET device. The high selectivity toward DA without interference of AA and UA resulted from the selective adsorption of DA on the surface of CPPy via $\pi-\pi$ interaction between the conjugated chains of PPy and the phenyl groups of DA.

H_2O_2, DA, AA, and UA can also be sensitively detected by corresponding enzymes (e.g., horseradish peroxidase for H_2O_2 and uricase enzyme for UA) immobilized in CP matrices. For example, a peroxidase/PPy nanotube composite-based H_2O_2 sensor showed an impressive sensitivity of 1 A M^{-1} cm^{-2} with a low detection limit (5 nM).[44] However, the short operational lifetime and poor reusability of biocatalysts limited their practical applications. Therefore, the no-enzymatic sensors described above are preferential choices for these electroactive molecules. On the other hand, for detecting nonelectroactive biomolecules such as glucose, cholesterol, and triglycerides, specific enzymes must be used. In the case of using a composite of CP and enzyme as sensing layer, the CP component usually acted as a mediator for transferring electrons from enzyme to substrate electrode.[65] The immobilization of enzymes into CP matrices can be performed by physical adsorption, covalent bonding, and electrochemical codeposition.[9] However, the first technique was tested to be less efficient, because the physically adsorbed enzyme molecules were possibly leached from the electrode surface during sensing process. Furthermore, nanostructured CPs usually have larger specific surface areas and higher conductivities than their films; thus they can immobilize more enzymes for electrocatalyzation. For example, recently, glucose oxidase (GOx) was directly entrapped into PEDOT during galvanostatic polymerization by using poly(L-lactide) nanofibers as a template to form a PEDOT NF-GOx composite on the Pt microelectrode arrays.[16] This electrode showed a high sensitivity of 9.2 μA cm^{-2} mM^{-1} for detecting glucose, and this value was 156% higher than that of a PEDOT film-GOx electrode prepared from the same system without using a template. The PEDOT NF matrix also slightly improved the stability of enzyme. However, the sensitivity of the PEDOT NF-GOx sensor at an operation potential of 700 mV vs Ag/AgCl decreased to 40% after storing at 4 °C in PBS for 30 days. This is mainly due to the decrease in the conductivity of PEDOT by the strong oxidant, H_2O_2.

In order to further enhance the sensitivity and stability of the CP/enzyme composite-based sensors toward nonelectroactive biomolecules, blending a precious metal catalyst is an effective approach.[21,45] A typical example is a PANI/Pt nanoparticles/GOx-based sensor reported by Yu et al.[45] A PANI gel film was grown on the surface of a GCE by drop casting a mixture of aniline monomer, phytic acid as a cross-linker and doping agent, and a polymerization initiator. Pt nanoparticles were

DOI: 10.1021/jacs.5b12474
J. Am. Chem. Soc. 2016, 138, 2868−2876

modified on the gel film by reducing chloroplatinic acid with formic acid, followed by covalently immobilizing GOx with a glutaraldehyde cross-linker (Figure 4d,e). This hybrid film modified electrode exhibited a high sensitivity of 96.1 μA cm^{-2} mM^{-1} and a fast response rate (~3 s) for detecting glucose (Figure 4f). This excellent sensing performance is partly attributed to the porous hydrophilic PANI matrix, facilitating the diffusion of H_2O_2 from the enzymatic reaction sites to Pt nanoparticles for further electrochemical oxidation. Furthermore, the high conductivity of this hydrogel film guaranteed the rapid charge transfer between enzyme and substrate electrode. Very recently, the same group also applied this three-component system (PANI/Pt/enzyme) for the detection of human metabolites including UA, cholesterol, and triglycerides, showing high sensitivities.[21]

3. CP-BASED PHOTOCATALYSTS

Semiconductors of metal oxides such as TiO_2 are widely used as photocatalysts.[66] However, they can absorb only ultraviolet (UV) light, accounting for 4% of solar energy. Visible light accounts for approximately 43% of solar energy, making the photocatalysts with activities under visible light of great practical importance. CPs usually have narrow bandgaps; thus they can absorb ultraviolet and visible lights. For example, the bandgaps of PANI, PPy, and PTh were reported to be 2.8, 2.2, and 2.0 eV, respectively. Their bandgaps can also be narrowed by chemical modification with different functional groups to extend their absorption ranges.[67] Thus, CP-based photocatalysts are workable upon excitation with visible light.

Catalysts for the Decomposition of Organic Pollutants. A few inherent CPs were reported to be promising photocatalysts for dye decomposition.[10,11] Upon excitation with light, CP catalyst absorbs light to induce $\pi-\pi^*$ electron transition. The excited electrons in the π^*-orbital of CP (lowest unoccupied molecular orbitals, LUMO) activate the adsorbed oxygen molecules to superoxide radicals ($O_2^{\bullet-}$) for oxidizing pollutants (Figure 5a).[11] The holes in the highest occupied molecular orbitals (HOMO) of CP can also directly oxidize the pollutants. In an early study, a 10 μm-thick poly(3-octylthiophene-2,5-diyl) film was used as a photocatalyst for the degradation of iprobenfos under visible light.[10] However, its photocatalytic performance was poor. This is probably due to the weak redox ability, fast recombination of photoelectrons and holes, and small specific surface area of this CP film. An ideal CP photocatalyst should have a narrow bandgap for absorbing solar light, a perfect conjugated structure for fast transfer of charge carriers, and a large specific surface area for the adsorbing target pollutants. Following these rules, in a very recent report, nanofibers of poly(diphenylbutadiyne) (PDPB) (inset of Figure 5b) were prepared by photopolymerization the monomer using a hexagonal mesophase soft template.[11] They have a bandgap of 1.81 eV, exhibiting strong catalytic activity for the degradation of model pollutants (phenol and methyl orange) under visible light (λ > 450 nm, 300 W xenon lamp), surpassing those of bulk PDPB and Ag modified P25 TiO_2 (Figure 5b). In this case, photogenerated $O_2^{\bullet-}$ radicals played a dominate role in the oxidation of pollutants. The PDPB nanostructures reduced the recombination of photogenerated electrons and holes because of their small dimensions and less defective chain structures.

The photocatalytic performances of traditional CPs such as PPy, PANI, and PTh are poor. Their performances can be greatly improved by the incorporation of semiconducting metal compounds (e. g., TiO_2, ZnO, CdS) to restrict the recombination of charge carriers. Actually, in this case, CPs acted as photosensitizers to absorb visible lights. The photocatalyzation mechanism of the composite catalysts was proposed as follows.[68] Taking PANI/TiO_2 as an example, visible light induced the $\pi-\pi^*$ electron transition of PANI. The excited electrons in the LUMOs of PANI chains were injected to the conduction bands (CB) of TiO_2 and then transferred to the surface of this composite catalyst to react with water and oxygen, forming $O_2^{\bullet-}$ radicals to oxidize organic pollutants (Figure 5c). To realize rapid charge transfer and efficient separation of electron−hole pairs, effective interfacial contacts between CP matrix and TiO_2 nanoparticles to form heterojunctions are important.[69] For example, a composite catalyst of TiO_2 nanoparticles modified with monolayer PANI was prepared by surface adsorption and its content of PANI was measured to be only 3% (by weight).[68] This PANI/TiO_2 composite can degrade methylene blue (MB, 10 mg L^{-1}) by 88% in 5 h and Rhodamine B (10 mg L^{-1}) by 97% in 100 min under visible light (λ > 450 nm, 500 W xenon lamp).

Except inorganic semiconductors, graphitic carbon nitride (g-C_3N_4) with a bandgap of 2.7 eV has also been blended into CPs to form composite photocatalysts. For example, a PANI-g-C_3N_4 composite photocatalyst was synthesized by "*in situ*" oxidative polymerization of aniline monomer in the presence of g-C_3N_4 particles.[13] This catalyst can degrade MB (10 mg L^{-1}) by 92.8% in 2 h under visible light (λ > 420 nm, 500 W xenon lamp).

Catalysts for Water Splitting. Splitting of water into hydrogen and oxygen gases can convert solar power to clean chemical energy.[70] The efficiency and rate of photocatalyzed water splitting are controlled by the efficiency of charge separation and the electrochemical properties of photocatalyst (driving force for proton reduction).[14] Generally, pure CPs are not able to photocatalyze water splitting because of the fast recombination of photogenerated charge carriers. Nevertheless, they can be used as sensitizers for other photocatalysts (e.g., TiO_2,[14] g-C_3N_4[12]) to improve their performances under visible light. Here, we take poly(3-hexylthiophene)/g-C_3N_4 (P3HT/g-C_3N_4) composite photocatalyst as an example.[12] Under visible light, photoinduced electrons in P3HT can be transferred to the CBs of g-C_3N_4, and the holes in g-C_3N_4 were transferred to the HOMOs of P3HT, driving the separation of charge carriers (Figure 5d). The electrons in g-C_3N_4 reduced the protons in water to hydrogen (H_2). However, the photocatalytic activity of CP/TiO_2 or CP/g-C_3N_4 was tested to be extremely low. To address this problem, an effective approach is blending a cocatalyst (e.g., Pt) and adding a sacrificial electron donor (or hole scavenger) into water. For example, the H_2 evolution rate in a pure water system was increased from 0.3 to 15 μmol h^{-1} by loading 3 wt % Pt on PPy/g-C_3N_4.[71] In the case of using P3HT/g-C_3N_4 with 1 wt % Pt as the photocatalyst and Na_2S and Na_2SO_3 as sacrificial electron donors, the H_2 evolution rate under visible light (λ > 400 nm, 300 W high-pressure mercury lamp) was measured to be as high as 560 μmol h^{-1}.[12]

4. CHALLENGES AND PROSPECTS

CP-based catalysts include inherent CPs, CP composites, and CP-derived heteroatom-doped carbons. They have been widely explored as electrocatalysts and photocatalysts, showing promising applications in DSSCs, fuel cells, electrochemical sensors, water splitting, and degradation of organic pollutants, etc. However, the catalytic mechanisms have not yet been

DOI: 10.1021/jacs.5b12474
J. Am. Chem. Soc. 2016, 138, 2868−2876

extensively revealed, and the practical applications of CP-based catalysts still face several challenges.

First, inherent CP catalysts and CP-derived heteroatom-doped carbons exhibited excellent catalytic performances in DSSCs and fuel cells. However, the exact catalytic sites of these catalysts and the catalytic mechanisms are still unclear, needing systematical studies. The performances of these catalysts strongly depend on their conductivities, specific surface areas, and electrochemical activities and stabilities. Thus, effective techniques for preparing CP nanostructures with excellent electrical and electrochemical properties are required. Second, CP-based composite catalysts usually have catalytic performances superior to their individual components because of synergetic effects. However, the precise controls in their compositions, microstructures, and interactions between different components are big challenges. Furthermore, expensive noble metals such as Pt and Au are frequently applied as the cocatalysts. Thus, a balance between cost and performance of a CP-based composite catalyst needs to be considered for practical application. Third, flexible and wearable energy and electronic devices have recently attracted a great deal of attention. CP films and their composites can be used as flexible and/or transparent catalytic electrodes in these devices. For these applications, the interfacial interactions between CP components and other functional materials require to be optimized. Effective techniques that can assemble CP-based devices with superelasticity, small sizes, and/or smart performances are expected. Fourth, recent advancements on CP-based photocatalysts are encouraging. However, the successful examples are still few, and the related researches are at an initial stage. Rational designs of CP chain structures and proper constructions of CP nanostructures are very important for achieving high-performance CP-based photocatalysts. Last but not the least, the stability of CP-based catalysts is an important parameter for evaluating their performances. Although, many CP-based catalysts work well in lab tests, they need to be systematically examined in complicated systems or under practical conditions. Especially, the lifetimes of CP-based photocatalysts are still unsatisfactory.

Nevertheless, CP-based catalysts are cheap, readily prepared, and scaled up to industrial levels. They possess unique 1D conjugated structures and excellent electrical, electrochemical, and optical properties, showing promising catalytic performances in a variety of devices and systems. Along with the progresses in understanding the catalytic mechanisms and breakthroughs in synthesizing CPs with few structural defects and ideal nanostructures, we believe CP-based catalysts have a bright future with wide practical applications.

AUTHOR INFORMATION

Corresponding Author

*gshi@mail.tsinghua.edu.cn

Notes

The authors declare no competing financial interest.

ACKNOWLEDGMENTS

This work was supported by the National Basic Research Program of China (973 Program, 2012CB933402) and the Natural Science Foundation of China (51433005).

REFERENCES

(1) Li, C.; Bai, H.; Shi, G. Q. *Chem. Soc. Rev.* **2009**, *38*, 2397.
(2) Heinze, J.; Frontana-Uribe, B. A.; Ludwigs, S. *Chem. Rev.* **2010**, *110*, 4724.
(3) Wu, M. X.; Ma, T. L. *J. Phys. Chem. C* **2014**, *118*, 16727.
(4) Yun, S. N.; Hagfeldt, A.; Ma, T. L. *Adv. Mater.* **2014**, *26*, 6210.
(5) Winther-Jensen, B.; MacFarlane, D. R. *Energy Environ. Sci.* **2011**, *4*, 2790.
(6) Hao, F.; Dong, P.; Luo, Q.; Li, J. B.; Lou, J.; Lin, H. *Energy Environ. Sci.* **2013**, *6*, 2003.
(7) Yuan, X. X.; Ding, X. L.; Wang, C. Y.; Ma, Z. F. *Energy Environ. Sci.* **2013**, *6*, 1105.
(8) Gerard, M.; Chaubey, A.; Malhotra, B. D. *Biosens. Bioelectron.* **2002**, *17*, 345.
(9) Cosnier, S.; Holzinger, M. *Chem. Soc. Rev.* **2011**, *40*, 2146.
(10) Wen, C.; Hasegawa, K.; Kanbara, T.; Kagaya, S.; Yamamoto, T. *J. Photochem. Photobiol., A* **2000**, *133*, 59.
(11) Ghosh, S.; Kouame, N. A.; Ramos, L.; Remita, S.; Dazzi, A.; Deniset-Besseau, A.; Beaunier, P.; Goubard, F.; Aubert, P. H.; Remita, H. *Nat. Mater.* **2015**, *14*, 505.
(12) Yan, H. J.; Huang, Y. *Chem. Commun.* **2011**, *47*, 4168.
(13) Ge, L.; Han, C. C.; Liu, J. *J. Mater. Chem.* **2012**, *22*, 11843.
(14) Dimitrijevic, N. M.; Tepavcevic, S.; Liu, Y.; Rajh, T.; Silver, S. C.; Tiede, D. M. *J. Phys. Chem. C* **2013**, *117*, 15540.
(15) Tran, H. D.; Li, D.; Kaner, R. B. *Adv. Mater.* **2009**, *21*, 1487.
(16) Yang, G.; Kampstra, K. L.; Abidian, M. R. *Adv. Mater.* **2014**, *26*, 4954.
(17) Pringle, J. M.; Armel, V.; MacFarlane, D. R. *Chem. Commun.* **2010**, *46*, 5367.
(18) Khomenko, V. G.; Barsukov, V. Z.; Katashinskii, A. S. *Electrochim. Acta* **2005**, *50*, 1675.
(19) Trevisan, R.; Doebbelin, M.; Boix, P. P.; Barea, E. M.; Tena-Zaera, R.; Mora-Sero, I.; Bisquert, J. *Adv. Energy Mater.* **2011**, *1*, 781.
(20) Lee, T. H.; Do, K.; Lee, Y. W.; Jeon, S. S.; Kim, C.; Ko, J.; Im, S. S. *J. Mater. Chem.* **2012**, *22*, 21624.
(21) Li, L. L.; Wang, Y. Q.; Pan, L. J.; Shi, Y.; Cheng, W.; Shi, Y.; Yu, G. H. *Nano Lett.* **2015**, *15*, 1146.
(22) Xiao, Y. M.; Lin, J. Y.; Tai, S. Y.; Chou, S. W.; Yue, G. T.; Wu, J. H. *J. Mater. Chem.* **2012**, *22*, 19919.
(23) Debe, M. K. *Nature* **2012**, *486*, 43.
(24) Lu, S.; Wang, S. S.; Han, R. B.; Feng, T.; Guo, L. J.; Zhang, X. H.; Liu, D. S.; He, T. *J. Mater. Chem. A* **2014**, *2*, 12805.
(25) Xia, J. B.; Masaki, N.; Jiang, K. J.; Yanagida, S. *J. Mater. Chem.* **2007**, *17*, 2845.
(26) Li, C. T.; Lee, C. P.; Fan, M. S.; Chen, P. Y.; Vittal, R.; Ho, K. C. *Nano Energy* **2014**, *9*, 1.
(27) Saito, Y.; Kitamura, T.; Wada, Y.; Yanagida, S. *Chem. Lett.* **2002**, 1060.
(28) Lu, C. Y.; Tsai, C. H.; Tsai, Y. T.; Hsu, C. J.; Chang, C. H.; Wu, C. C. *Adv. Energy Mater.* **2015**, *5*, 1401738.
(29) Chen, P. Y.; Li, C. T.; Lee, C. P.; Vittal, R.; Ho, K. C. *Nano Energy* **2015**, *12*, 374.
(30) Sudhagar, P.; Nagarajan, S.; Lee, Y. G.; Song, D.; Son, T.; Cho, W.; Heo, M.; Lee, K.; Won, J.; Kang, Y. S. *ACS Appl. Mater. Interfaces* **2011**, *3*, 1838.
(31) Xu, H. X.; Zhang, X. Y.; Zhang, C. J.; Liu, Z. H.; Zhou, X. H.; Pang, S. P.; Chen, X.; Dong, S. M.; Zhang, Z. Y.; Zhang, L. X.; Han, P. X.; Wang, X. G.; Cui, G. L. *ACS Appl. Mater. Interfaces* **2012**, *4*, 1087.
(32) Tsao, H. N.; Burschka, J.; Yi, C.; Kessler, F.; Nazeeruddin, M. K.; Graetzel, M. *Energy Environ. Sci.* **2011**, *4*, 4921.
(33) Winther-Jensen, B.; Winther-Jensen, O.; Forsyth, M.; MacFarlane, D. R. *Science* **2008**, *321*, 671.
(34) Bashyam, R.; Zelenay, P. *Nature* **2006**, *443*, 63.
(35) Choi, C. H.; Park, S. H.; Woo, S. I. *ACS Nano* **2012**, *6*, 7084.
(36) Zhang, J. T.; Zhao, Z. H.; Xia, Z. H.; Dai, L. M. *Nat. Nanotechnol.* **2015**, *10*, 444.
(37) Meng, Y. Y.; Voiry, D.; Goswami, A.; Zou, X. X.; Huang, X. X.; Chhowalla, M.; Liu, Z. W.; Asefa, T. *J. Am. Chem. Soc.* **2014**, *136*, 13554.
(38) Liang, H. W.; Wei, W.; Wu, Z. S.; Feng, X.; Müllen, K. *J. Am. Chem. Soc.* **2013**, *135*, 16002.

DOI: 10.1021/jacs.5b12474
J. Am. Chem. Soc. 2016, 138, 2868−2876

(39) Ding, W.; Li, L.; Xiong, K.; Wang, Y.; Li, W.; Nie, Y.; Chen, S. G.; Qi, X. Q.; Wei, Z. D. *J. Am. Chem. Soc.* **2015**, *137*, 5414.
(40) Wu, G.; More, K. L.; Johnston, C. M.; Zelenay, P. *Science* **2011**, *332*, 443.
(41) Feng, X. M.; Mao, C. J.; Yang, G.; Hou, W. H.; Zhu, J. J. *Langmuir* **2006**, *22*, 4384.
(42) Lin, K. C.; Tsai, T. H.; Chen, S. M. *Biosens. Bioelectron.* **2010**, *26*, 608.
(43) Lee, J. S.; Oh, J.; Kim, S. G.; Jang, J. *Small* **2015**, *11*, 2399.
(44) Ekanayake, E.; Preethichandra, D. M. G.; Kaneto, K. *Sens. Actuators, B* **2008**, *132*, 166.
(45) Zhai, D. Y.; Liu, B. R.; Shi, Y.; Pan, L. J.; Wang, Y. Q.; Li, W. B.; Zhang, R.; Yu, G. H. *ACS Nano* **2013**, *7*, 3540.
(46) Gratzel, M. *Nature* **2001**, *414*, 338.
(47) Tai, Q. D.; Chen, B. L.; Guo, F.; Xu, S.; Hu, H.; Sebo, B.; Zhao, X. Z. *ACS Nano* **2011**, *5*, 3795.
(48) Biallozor, S.; Kupniewska, A. *Electrochem. Commun.* **2000**, *2*, 480.
(49) Chen, J. G.; Wei, H. Y.; Ho, K. C. *Sol. Energy Mater. Sol. Cells* **2007**, *91*, 1472.
(50) Xia, Y. J.; Sun, K.; Ouyang, J. Y. *Energy Environ. Sci.* **2012**, *5*, 5325.
(51) Kim, N.; Kee, S.; Lee, S. H.; Lee, B. H.; Kahng, Y. H.; Jo, Y. R.; Kim, B. J.; Lee, K. *Adv. Mater.* **2014**, *26*, 2268.
(52) Zhang, M.; Yuan, W. J.; Yao, B. W.; Li, C.; Shi, G. Q. *ACS Appl. Mater. Interfaces* **2014**, *6*, 3587.
(53) Zhou, Q. Q.; Chen, S.; Zhang, M.; Wang, L. D.; Li, Y. R.; Shi, G. Q. *Chin. J. Chem.* **2016**, *34*, 59.
(54) Hong, W. J.; Xu, Y. X.; Lu, G. W.; Li, C.; Shi, G. Q. *Electrochem. Commun.* **2008**, *10*, 1555.
(55) Yun, S. N.; Liu, Y. F.; Zhang, T. H.; Ahmad, S. *Nanoscale* **2015**, *7*, 11877.
(56) Nie, Y.; Li, L.; Wei, Z. D. *Chem. Soc. Rev.* **2015**, *44*, 2168.
(57) Birry, L.; Zagal, J. H.; Dodelet, J. P. *Electrochem. Commun.* **2010**, *12*, 628.
(58) Gong, K. P.; Du, F.; Xia, Z. H.; Durstock, M.; Dai, L. M. *Science* **2009**, *323*, 760.
(59) Wang, X. L.; Shi, G. Q. *Phys. Chem. Chem. Phys.* **2015**, *17*, 28484.
(60) Lai, L. F.; Potts, J. R.; Zhan, D.; Wang, L.; Poh, C. K.; Tang, C. H.; Gong, H.; Shen, Z. X.; Lin, J. Y.; Ruoff, R. S. *Energy Environ. Sci.* **2012**, *5*, 7936.
(61) Fan, X. B.; Zhang, G. L.; Zhang, F. B. *Chem. Soc. Rev.* **2015**, *44*, 3023.
(62) Li, Q.; Cao, R. G.; Cho, J.; Wu, G. *Adv. Energy Mater.* **2014**, *4*, 1301415.
(63) Masa, J.; Xia, W.; Muhler, M.; Schuhmann, W. *Angew. Chem., Int. Ed.* **2015**, *54*, 10102.
(64) Jahnke, H.; Schonborn, M.; Zimmermann, G. *Top. Curr. Chem.* **1976**, *61*, 133.
(65) Wang, Z. Y.; Liu, S. N.; Wu, P.; Cai, C. X. *Anal. Chem.* **2009**, *81*, 1638.
(66) Ma, Y.; Wang, X. L.; Jia, Y. S.; Chen, X. B.; Han, H. X.; Li, C. *Chem. Rev.* **2014**, *114*, 9987.
(67) Roncali, J. *Chem. Rev.* **1997**, *97*, 173.
(68) Zhang, H.; Zong, R. L.; Zhao, J. C.; Zhu, Y. F. *Environ. Sci. Technol.* **2008**, *42*, 3803.
(69) Wang, H. L.; Zhang, L. S.; Chen, Z. G.; Hu, J. Q.; Li, S. J.; Wang, Z. H.; Liu, J. S.; Wang, X. C. *Chem. Soc. Rev.* **2014**, *43*, 5234.
(70) Qu, Y. Q.; Duan, X. F. *Chem. Soc. Rev.* **2013**, *42*, 2568.
(71) Sui, Y.; Liu, J. H.; Zhang, Y. W.; Tian, X. K.; Chen, W. *Nanoscale* **2013**, *5*, 9150.

DOI: 10.1021/jacs.5b12474
J. Am. Chem. Soc. 2016, 138, 2868−2876